Environmental Earth Sciences (2020) 79:114
https://doi.org/10.1007/s12665-020-8860-5

ORIGINAL ARTICLE

# Vulnerability assessment of flash floods in Wadi Dahab Basin, Egypt

**Maria Prama[1] · Adel Omran[2,3] · Dietrich Schröder[1] · Abdou Abouelmagd[4]**

Received: 7 March 2019 / Accepted: 2 February 2020 / Published online: 28 February 2020


## Abstract

Floods are considered one of the most severe natural disasters worldwide. They impact vast areas, particularly in arid/semi-arid regions, causing serious damages with thousands of human casualties and billions of Euros in economic losses. This study contributes to a comprehensive evaluation of flash flooding occurrences, impacts, and possible mitigation. In this study, The Dahab region in southern Egypt's Sinai Peninsula was selected for flash flooding vulnerability assessment. Although located in an arid region, it suffers from frequent and severe flash floods. Here, a straightforward workflow was applied to simulate the impact of flash flooding and assess the vulnerability of the Dahab area via consideration of a maximum storm event as a worst- case scenario. Originally, morphometric analysis was performed to determine the most hazardous sub-basins susceptible to flash flooding. The highest recorded storm event in the region was selected to calculate the maximum volume of surface runoff for the model simulation. Then, the hydrologic model and River Analysis System (HEC-RAS) software were used to calculate the inundation level across the entire city of Dahab. Despite some data limitations, this study shows clearly that the Dahab area would have problems incurring from flash flooding if no mitigation measures were to be considered. Results indicate that the area of Dahab is greatly vulnerable to flash flooding with approximately 72% of the total infrastructure being negatively impacted in the worst-case scenario. The adopted approach used in this study can be applied efficiently in similar regions in the Sinai Peninsula or elsewhere.

**Keywords** GIS · Flash floods · Vulnerability · Morphometric analysis · Hydrological model · HEC-RAS · Dahab city · Sinai Peninsula

## Introduction

Natural hazards are naturally occurring events having a negative impact on people and the environment. When a natural hazard threatens human life, damages properties, or has other negative effects on the human-populated environment so that it can no longer be handled locally, then it becomes designated as a natural disaster. Such disasters are combinations of exposure, vulnerability, and insufficient capacity to reduce or cope with the potential negative consequences (UNISDR 2009). Among natural disasters, floods are one of the most severe and, well known for thousands of human casualties plus causing billions of Euros in economic damage in many countries throughout the world. Floods are responsible for 44% of the deaths caused by natural hazards world-wide, especially in arid regions (Davies 2014). In these areas, flash floods are most likely to cause the most severe damages. Flash flooding is a surface water response to rainfall from intense thunderstorms or caused by a sudden release of water from a reservoir. This usually occurs with

✉ Adel Omran
adelfouad.omran@suezuniv.edu.eg

Maria Prama
maria.prama@konstanz.de

Dietrich Schröder
dietrich.schroeder@hft-stuttgart.de

Abdou Abouelmagd
abdou_abouelmagd@science.suez.edu.eg

[1] Department of Photogrammetry and Geoinformatics, Faculty Geomatics, Computer Science and Mathematics, Hochschule für Technik Stuttgart, Stuttgart, Germany

[2] Department of Science and Mathematical Engineering, Faculty of Petroleum and Mining Engineering, Suez University, Suez, Egypt

[3] Heidelberger Akademie Der Wissenschaften, Geography Institute, Tübingen University, Tübingen, Germany

[4] Department of Geology, Faculty of Science, Suez Canal University, Ismailia 41522, Egypt

a short lead time and frequently has considerable potential for damage resulting from high flow velocities and thus high hazard intensities (Hong et al. 2012).

There are many examples demonstrating the effects of flash floods in arid and semi-arid regions. Such regions cover approximately one-third of the world's land surface (Wagener et al. 2007). In Jordan, it has been reported that a flash flooding event occurred in March 1966 that led to about 200 deaths and 250 injuries. In addition to 3000 people being rendered homeless, approximately half of the buildings in the Ma'an town were destroyed (Al-Qudah 2011). In Saudi Arabia, more than 113 people lost their lives and 10,000 homes were destroyed because of catastrophic flash flood events in the last 5 years (Youssef et al. 2016). Such tragic events have motivated us to conduct this study in order to assess the flash floods that frequently hit the southeast coast of the Sinai Peninsula threatening the people and infrastructure of the Dahab area.

The city of Dahab is located in the southern mountainous terrain of the Sinai Peninsula about 600 km from Cairo. It is well documented that flash floods in this mountainous arid region are quite common and they are responsible for a large number of deaths and property damages (Abdalla et al. 2014). The potentiality of a flash flood for a certain hydrographic basin can be evaluated by calculating different morphometric parameters (Strahler 1964; Abdalla et al. 2014). Risks of flash floods have been assessed using geomorphometric analyses (e.g., Sujatha et al. 2013; Bhatt and Ahmed 2014; Farhan et al. 2016; Abdel-Fattah et al. 2017). In this context, morphometry refers to the measurement of the earth's surface area, landform dimensions, and shape. A detailed morphometric analysis of watersheds is capable of exploring the geomorphic history and the development of the drainage network (Farhan et al. 2016). It enhances the understanding of the hydrological processes and characteristics of the related sub-basins (Pal et al. 2012; Hajam et al. 2013). Furthermore, the morphometric analysis is applied to estimate the sub-catchments predominantly responsible for flash floods in a hydrographic basin (Bhatt and Ahmed 2014). Nowadays, geospatial analytical techniques—fully supported by GIS and remote sensing software—provide a powerful and convenient tool for conducting a morphometric analysis (Rahman et al. 2015).

In concert with the geomorphology, climate and land-use contribute dramatically to the occurring of flash floods. In addition, climate change will lead to higher chances of flash flood occurrences and thus increase the risk upon settlements in the affected regions (Kundzewicz and Kaczmarek 2000; Wagener et al. 2007). Moreover, impervious surface layers, which can be found in these regions, making them more vulnerable to flash flood impacts (Wicht and Skotak 2016). In recent studies, hydrologic models have played an important role in flood risk management, particularly in arid and semi-arid regions (Hagras et al. 2013; Jin et al. 2015). By means of such models, hydrological parameters can be estimated such as flow discharge and volume quantities serving to better evaluate the degree of flash flood risk. Different hydrological models have been used as an early warning system for flash floods in Egypt and elsewhere (Windarto 2010; Vanderkimpen et al. 2010; Cools et al. ; 2012). The flood early warning system plays an important role in decreasing the impact of flash floods. Another type of hydrological model is based mainly on the rainfall-runoff estimates. This type of model basically quantifies the probable severity of a flash flood and then identifies the possible vulnerability levels (Kim and Choi 2011). The Hydrologic Engineering Centre Hydrologic Modeling System (HEC-HMS) is considered a significant tool for simulating the precipitation-runoff processes of dendritic watershed systems and for calculating the volume of runoff released by a watershed (Adib et al. 2010; Scharffenberg 2004). The HEC-HMS model was designed for flow simulation based on three main components: the basin surface area, the prevailing climatic conditions, and the control indices. It has been applied to a variety of problems in a wide range of basins with different characteristics (Nandalal and Ratnayake 2010; Neto et al. 2014; Koneti et al. 2018). Such a model is capable of running a flood simulation and calculating hydrographs even for ungauged basins (e.g., Gumindoga et al. 2016).

A vulnerability assessment is an important step for ensuring the safety of people and properties in urban areas (Nasiri et al. 2016). Vulnerability is defined as the potentiality of a hazard and the characteristics of a community, a system, or an asset that makes it susceptible to the damaging effects of the hazard. The overall vulnerability of a community can be determined by assessing physical, social, economic, and environmental damage occurring from a potential hazard (UNISDR 2009). The physical vulnerability can be defined as contemplating only the structural damages (Mazzorana et al. 2014). In contrast, the economic vulnerability considers direct and indirect monetary losses through property damage, while, the environmental vulnerability addresses the impacts on the environment such as water and soil pollution – such as the removal of soil as well as plants and wildlife. Generally, the vulnerability as a term is related to the negative effects of natural hazards. These effects are generally measured in terms of damage or loss, either on an ordinal scale based on social values or perceptions and evaluations, or on a metric scale, such as in monetary units (Karagiorgos et al. 2016). There are two main diverse directions for vulnerability concepts, these being social science and natural science concepts (Fuchs 2009). In this study, land-use, hydrological, and topographical data were used to implement an assess of the physical and environmental vulnerability over the area of Dahab. Other social concepts were neglected due to the shortage of data availability.

The ultimate goal of this study was to assess flooding impacts on localities with concentrated populations including the infrastructure of these urban areas such as roads and buildings. This assessment was supported by the implementation of a workflow for estimating the vulnerability of flood hazard areas. A hazard map, based on a morphometric analysis and geomorphological parameter calculations, showed the potentiality of flash floods. For this analysis, a GIS model for creating the stream flow based on Digital Elevation Model (DEM) was used (Omran et al. 2016). In the following step, a hydrological model was applied to calculate surface runoff and the discharge volume of flash flood water. The resulting flood simulation showed the affected areas. Based on the results, an inundation flood map was created for the urbanized areas of the study area. Then, a land-use map was prepared to overlay the inundation flood map for assessing the physical vulnerability.

It is worth mentioning that this study is conducted based on limited available data sources. Because of an inadequate density of monitoring systems locations, the capacity for robust estimation and timely description of hydrological events such as flash flooding is severely limited. As such, our approach introduces the required tool to overcome this shortage in the arid environments by exploiting relevant data sources including topographic maps and digital data sets acquired from satellite-based remote sensing. Together with output from hydrological models, this combination provides the information necessary to achieve the goal of this study. Last, but not least, this study serves as a benchmark assessment and provides a methodology for flash flooding assessment that could be expanded across comparable regions in Egypt and elsewhere.

## Site description

The city of Dahab is located on the Gulf of Aqaba along the south-eastern coast of the Sinai Peninsula (Fig. 1). It has an area of about 1130 km$^2$ and is located at the downstream "mouth" of a large hydrographic basin called Wadi Dahab Basin (WDB), both city and basin cover a combined area of about 2086 km$^2$. Geomorphologically, the WDB can be divided into seven major sub-basins (in order by decreasing surface area): Wadi Zaghraa, Wadi Rimthy, Wadi Nasab, Wadi Saal, Wadi El-Genah, Wadi El Ghaieb and Wadi Abu Khshieb (Fig. 2). These sub-basins carry a tremendous amount of water during flood seasons that flow through high steep sloped rocky ravines with destructive speed and

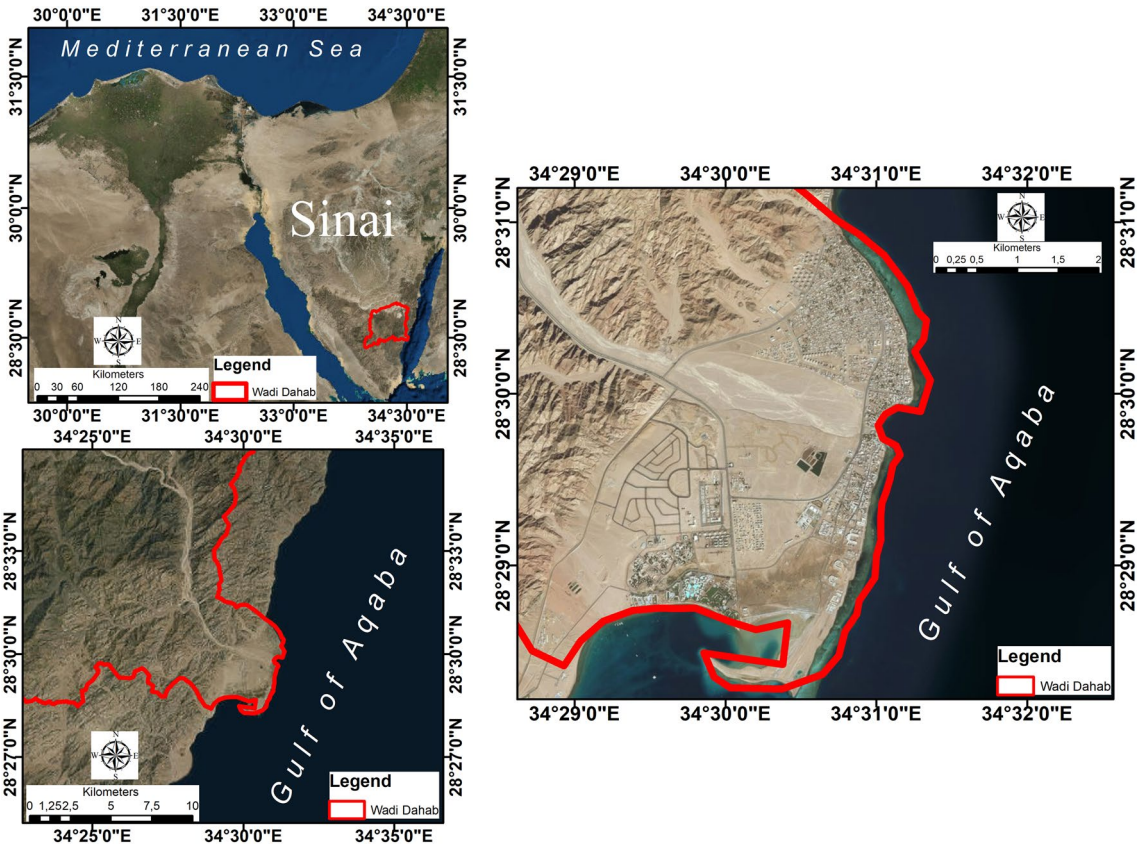


**Fig. 1** Location map of Wadi Dahab Basin (WDB) and its urbanized area in the city of Dahab (Google Earth 2017)

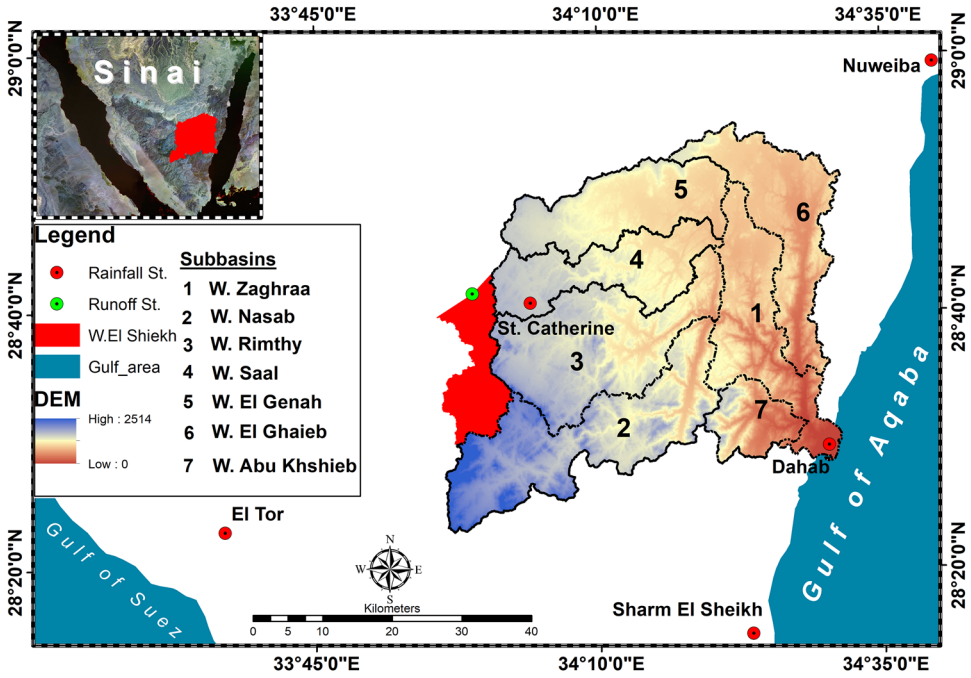


**Fig. 2** Hydrographic basins of WDB delineated over raster images of the Shuttle Radar Topography Mission (SRTM). The seven sub-basins comprising the WDB and including Wadi El-Sheikh sub-basin (in Red) for model calibration

feed the outlet of the basin that surrounds the city of Dahab (SSRDP 2006). Dahab represents a world-renowned area, especially for its golden sandy beaches and attractive diving activities in the presence of beautiful coral reefs and rare marine species. It is also considered an emerging and developing city in the southern Sinai Governorate with promising economic prospects, tourist destination, and growing urbanization. The climate of the area has been classified as a typical desert hyper-arid (Lin 1999), where it receives an average annual rainfall ranging from about 10 mm near the coast and increasing to about 50 mm in the highland catchment areas (Omran 2013). Although receiving such little rainfall, the Dahab area has recently witnessed frequent events of severe flash flooding that primarily originated from the nearby mountainous catchment areas.

The most devastating flash floods were recorded during the following rainfall events: May 1976, October 1987, November 1996, January 2010, and October 2016 (Cools et al. 2012). The latest flash flood was catastrophic causing 26 deaths, 72 injured, and 6500 families affected (OCHA 2016). No doubt that global climate change has a significant impact on the frequency and magnitude of the flash flood events. In southern Sinai, the frequency of the rainfall is already very low with recorded rainy storm events that are usually only occurring once per year. However, during the past 5 years, the area was subjected to more than two rainy storm events per year. These events can be considered alarming threats to the settlements and lives that are located at the downstream openings of the Sinai Mountain valleys (Crane 2015). During the last years of the twentieth century, the Egyptian government constructed many projects for increasing and improving both services and facilities within the city of Dahab in order to accommodate the increasing number of tourists as well as the local residents, and to aid in the development of the city. According to the population projection of the South Sinai Environmental Action Plan, Dahab has a population of approximately 31,700 residents in 2017, representing about 11% of the total population in the south Sinai (SSRDP 2006).

## Data and methods

### Data sources

The data used in this study were collected from different sources: (1) topographic maps of southern Sinai with a scale of 1:50,000 were acquired from the Egyptian Military Survey Department; (2) a digital elevation model (DEM) was provided by the Shuttle Radar Topography Mission (SRTM) with 30 m resolution. The SRTM data were downloaded from the NASA's distributed active archive system (DAAC), located at https://daac.gsfc.nasa.gov; (3) meteorological data were obtained from the Egyptian Meteorological Authority (EMA), and (4) Google Earth images were used for land-use mapping. All data were processed using commercial, public domain, and open source software (e.g., ArcGIS, QGIS, and HEC-HMS). Model parameters were calibrated, and results were validated against field data and data published in the internal and technical reports (SSRDP 2006; Omran 2013).

## Morphometric analysis

Figure 3 shows the workflow used for flood vulnerability assessment in the area of Dahab. First, a morphometric analysis was achieved using the acquired SRTM-DEM for delineating the hazardous sub-basins located in the upstream areas of the WDB. Such DEM has been proven to be very useful for calculating both geomorphological parameters (e.g., slopes, slope length, slope shape, and slope aspects) and hydrologic parameters (e.g., flow direction, flow accumulation, watershed delineation, stream networks, and flow length) (Ludwig and Schneider 2006, Sharma and Tiwari 2014). The hydrology toolbox of ArcGIS was used to delineate and extract the drainage network of the WDB.

Before starting the drainage network extraction, a fill processing was applied to remove the existing sinks in the DEM. Then, a flow direction raster was created by applying the D8-method (Jenson and Domingue 1988). Finally, different layers of the flow accumulation, stream link, and drainage network were generated using the stream ordering tool. The stream ordering technique used here is based on the work proposed and described by (Strahler 1957; 1964). This technique assigns a numerical value to each stream and builds a hierarchical relation between streams (Pierson et al. 2008). The watershed delineation tool requires pour point digitization before delineating the sub-basins (Omran et al. 2011). The workflow was applied from DEM processing to the extraction of morphometric parameters to larger regions, where perhaps hundreds of watersheds have to be delineated and classified. Although the complete process was implemented straightforwardly on DEM, the extracted results still retain different problems regarding their credibility in using the data in geomorphological and hydrological models.

Fieldwork still forms one of the most precise approaches to validate the channel network (Chorley et al. 1984). The exact stream network can be examined in the field, but the time and effort required make it impractical to check for stream validity, especially in large-scale catchments. To accomplish stream network validity, topographic maps were considered. Based on the geodetic field survey, drainage networks were captured accurately and were mapped following the cartographic rules of generalization, depending on the scale of the map. On the other hand, the details of the drainage network extracted from a DEM are closely related to the

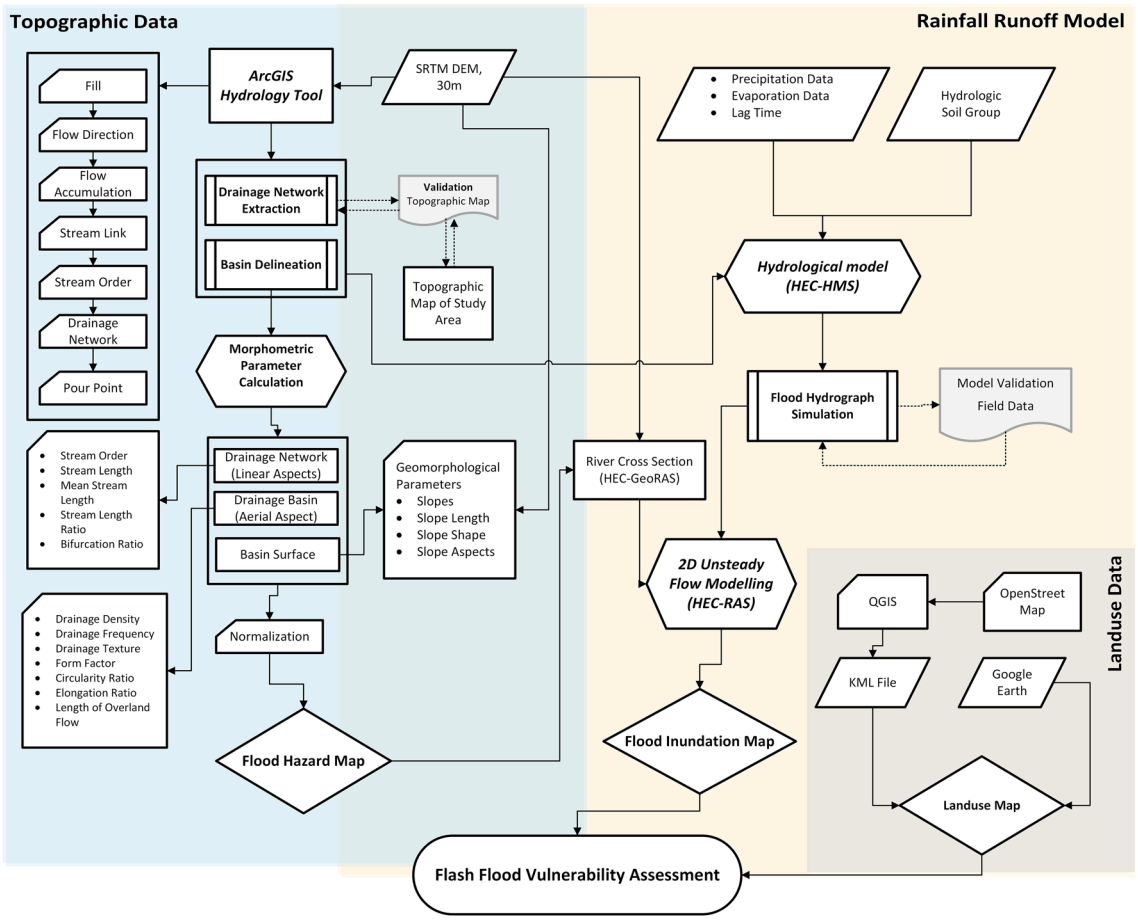


**Fig. 3** Workflow of flood vulnerability assessment of the city of Dahab

DEM's resolution. For a plausibility check, the extracted number of streams according to their order were compared with the streams extracted from the available topographic maps (scale 1:50,000), with six topographic maps covering the entire area of the WDB.

After extracting the drainage network, the corresponding watersheds were delineated. Basically, the location of the outlet defines the area of the watershed. Thus, the most important aspect for defining and delineating a watershed is to fix the outlet of the drainage course. It is worth mentioning that the total number of streams for each order should have the same number for the delineated basins. So, using the DEM in lieu of topographic maps was advantageous because of its ability to delineate the basins of small orders (i.e., 1st, 2nd and 3rd). Furthermore, data obtained from the DEM regarding the small basins such as basin area and perimeter were useful in the hydrological modeling. These data are not easily derived using the topographic maps.

To understand the relationship between different drainage patterns, morphometric parameters were carefully analyzed with respect to linear and aerial aspects. Basically, the linear aspects reflect the topological character and pattern of the drainage channel. Such aspects include stream order, stream length, mean stream length, stream length ratio, and bifurcation ratio. The area of basins directly affects the peak flow, surface runoff, and storm hydrograph. On the other hand, the aerial aspects deal with the total area of the basins that are contributing to flooding. Morphometric parameters that are associated with aerial aspects are drainage density, stream frequency, texture ratio, form factor, circulatory ratio, elongation ratio, length of overland flow, and shape factor. The evaluation of the linear aspect started with ordering the stream network. The size of the stream network and a basin surface area is primarily dependent on the stream order (Palaka 2014).

The morphometric parameters were calculated using the formulas presented in the work of (Parveen et al. 2012; Waikar and Nilawar 2014; Rahman et al. 2015) to identify the topographical surface characteristics that affect the dynamic surface runoff indirectly. Additionally, the hazardous flood risk for each sub-basin was assessed based on the relationship between the parameter values and the risk of flash flood as follows: Group (1) comprises parameters of stream order, stream frequency, stream density, circularity ratio, form factor, and texture ratio. They all have a direct proportional impact on the flash flooding susceptibility. Group (2) comprises parameters of bifurcation ratio, elongation ratio, shape factor, and length of overland flow that all are inversely proportional to the flash flooding susceptibility. The quantitative values associated with each type of parameter were interpreted as score values related to the flooding risk. An overlay operation was used to get the sum of scores for each sub-basin which was then used as a relative measure of the potential for flash flooding. The score values for each parameter were calculated using a simple statistical approach (Abuzied et al. 2016; Youssef et al. 2016; Pradhan 2010; Omran 2013). To present a flood hazard risk map, results were classified into three different categories using equal intervals (low risk, medium risk, and high risk). The raw score for each parameter was normalized using Eq. (1), taking into consideration the different signs of each parameter as well:

$$X_{\mathrm{j}} = \frac{\left(R_{\mathrm{j}} - R_{\min}\right)}{\left(R_{\max} - R_{\min}\right)}, \tag{1}$$

where $X_{\mathrm{j}}$ is the normalized score; $R_{\mathrm{j}}$ is the raw score; $R_{\min}$ and $R_{\max}$ are the minimum and maximum score, respectively.

Last, a flood hazard map was generated using the unweighted sum of all normalized morphometric risk parameters.

## Hydrological modeling

After defining the hazardous regions (i.e., sub-basins) based on the morphometric parameters, a hydrological model simulation was implemented to determine the maximum volume of the surface runoff in the WDB. For such simulation, the Hydrologic Engineering Centre-Hydrologic Modeling System (HEC-HMS) software was used. The model implemented in HEC-HMS is designed to simulate the hydrological processes of hydrographic basins. It has been proved to give accurate results in predicting watershed response, particularly those resulting from storm events (Choudhari et al. 2014). The HEC-HMS is basically a combination of a basin model, a meteorological model, a tool for processing time-series data, and control specifications. The model is designed for the physical representation of watersheds, considering hydrologic elements, and the calculations to simulate the physical processes. The extracted drainage network and the delineated basins from the morphometric analysis were used as input parameters for this model.

The Soil Conservation Service Curve Number (SCS-CN) method was used to calculate the output parameters such as the infiltration volume and the surface runoff within a basin. The SCS-CN method was developed by the US Department of Agriculture (USDA), Soil Conservation Service and it has been widely applied to predict the volume of direct surface runoff from a specific rainfall (Mockus 1972). The curve number (CN) is an empirical parameter used in hydrology for predicting runoff and was developed by USDA (USDA-SCS 1985). The challenge of this method was the selection of the value related to the CN and assigning the initial abstraction ratio. This ratio is defined as the maximum absorption amount of the rainfall before the onset of surface runoff (Patel 2016). The value of the CN was determined

based on the land-use, the hydrological conditions, and the hydrological soil type (Abuzied et al. 2016). A single CN value was used to compute the rainfall excess at the outlet of the catchments. The higher the CN value, the higher the runoff potential (Adham et al. 2014).

The WDB can be categorized as a desert area and its ground coverage has rock cover, litter, grass, and brush overstory (SSRDP 2006). More than 85% of the study area of WDB is composed of basement rock and sedimentary limestone giving the study area an infiltration rate of both rock types ranging from 1.7 to 3.4 mm per hour (Omran 2013). These types of rock represent the main catchment soil cover across the boundary of WDB. Regarding the soil type, it has been found that the hydrological soil class of WDB is type "C" (USDA 1993). Such a class means that the soil has a minimum infiltration rate of 1.3–3.8 mm per hour; this characterizes soils having a slow water transmission rate and high runoff potentiality. Abuzied et al. (2016) stated that the CN value for the basin of Wadi Watir, located at the north of the WDB, ranges from 83.33 to 92.02. As there is a similarity of bedrocks and infiltration conditions between both basins (i.e., W. Dahab and W. Watir) combined with a large extensive coverage of the same soil class 'C' in WDB, a CN value was assigned for the WDB with similar range as applied in Wadi Watir. The initial abstraction ratio ($I_a$) can be calculated using the following formula (USDA 1986):

$$I_a = 0.2\,S, \tag{2}$$

where $I_a$ is the initial abstraction ratio and $S$ is the potential retention (i.e., storage). Here, 0.2 is a constant value of the initial abstraction parameter (Noori et al. 2011). The relationship between the CN and $S$ can be seen in the following equation (USDA 1986):

$$S = \frac{1000}{\mathrm{CN}} - 10, \tag{3}$$

with $1 \leq \mathrm{CN} \leq 100$.

Another important input parameter for the hydrological modeling is the rainfall data. The rainfall is certainly one of the primary factors for occurring flash floods, where most of the rainfall events in the study area occur during the winter season. The climatological records of Egypt indicate that the intensity of the rainfall events during autumn and spring are sometimes large enough to create destructive flash floods, particularly in the southern part of Egypt and Sinai Peninsula (SSRDP 2006). The average monthly rainfall over the study area during the rainy season in winter (i.e., November–March) ranges between 4.7 and 23.4 mm (Omran 2013). The average values of rainfall increase over the northern, southern, and western terrains of the WDB because of its elevated topography. Five meteorological stations are located close to the study area, namely Saint Catherine, Sharm El-Sheikh, Nuweiba, Dahab, and El-Tur. Unfortunately, all of these stations have intermittent records throughout the previous years except the station at Saint Catherine.

In this study the rainfall records retrieved from Saint Catherine station were used for the following reasons: (1) the majority of the rainfall events were recorded at this station for a long time (1937 to present), (2) the station is located at higher elevation compared to other stations in the region, about 1350 m above mean sea level, and (3) it is the nearest station to the WDB being adjacent to the western boundary of the basin as seen in Fig. 2. The meteorological station at Saint Catherine recorded the average annual rainfall during the rainy season with a value of 64.2 mm from (1970 to 2012), whereas the highest recorded rainfall event with 72.6 mm/day was on November 8th, 1937 (Fig. 4a). This value represents the maximum recorded rainfall amount in this region. The maximum precipitation per day might be repeated more than once during the next period of rainy seasons. Therefore, extreme value theory can help to estimate the chance of an event occurring during a given period of time. For this purpose, only the maximum daily record storm per year for Saint Catherine station (ranging seventy years from 1934 to 2016) was used (Fig. 4b). Additionally, an available highest storm (72.6 mm/day) hyetograph was constructed based on the only available hourly rainfall measurement for this maximum event and was used with the simulation of the hydrological model (Fig. 4c).

The evaporation rate is considered one of the primary loss factors thereby helping to determine the rainfall excess and the surface runoff in the hydrological model. The evaporation data were collected from a period ranging from 1934 to 2004 for three meteorological stations only, namely Saint Catherine, Sharm El-Shiekh, and El-Tur (Table 1). They are covering the southern, western, and south-western regions of the WDB, respectively. The evaporation data represent the mean daily evaporation rate, expressed as mm/day. The data show that the high mean evaporation rate occurs in summer months ranging from 11.1 to 26.8 mm/day. This mean decreases in winter months ranging from 5.7 to 16.4 mm/day. Interestingly, the total evaporation losses differ during storm months. The evaporation rate during the rainfall storms is lower than any other time during the year; therefore, the evaporation at the time of rain is small and its effect is limited. As an outcome of the lack of a measured evaporation rate for the maximum storm event at Saint Catherine, a constant evaporation rate was used for the simulated maximum rainy storm. The selected mean daily evaporation value was 6.9 mm/day (Table1); this is approximately equal to 0.2 mm/h at Saint Catherine station in November.

Once the flood event was simulated using the HEC-HMS, a model verification step was performed to check its results. The aim of this step was to calibrate the input parameters by

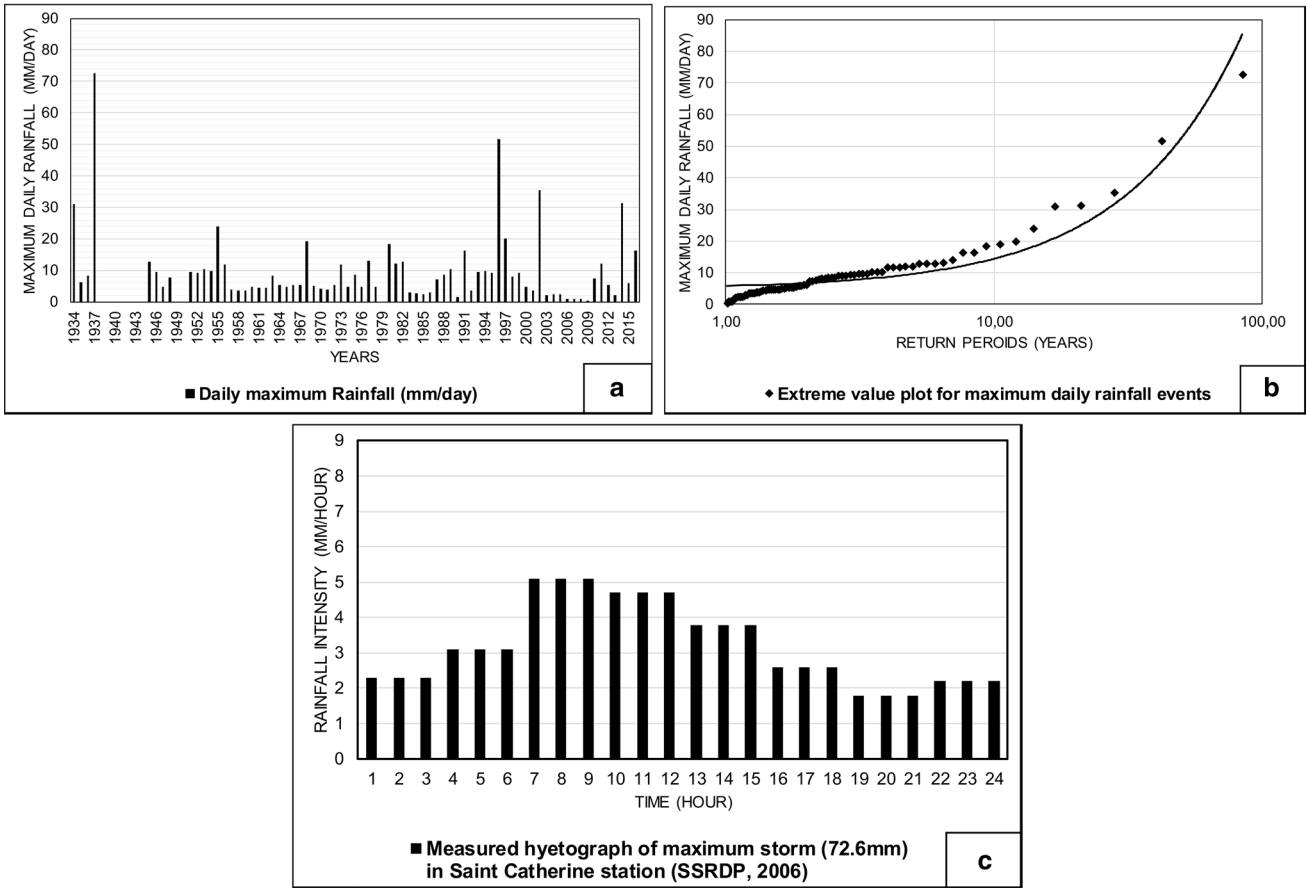


**Fig. 4** **a** Maximum daily storm recorded at Saint Catherine station from (1934–2016). **b** Extreme value plot for maximum daily rainfall events. **c** Measured hyetograph of maximum storm (72.6 mm) in Saint Catherine station (SSRDP 2006)

**Table 1** Mean daily evaporation (mm/day) for the period 1934–2004 (Egyptian Meteorological Authority 2008)

| | Jan | Feb | Mar | Apr | May | Jun | Jul | Aug | Sep | Oct | Nov | Dec | Average |
|---|---|---|---|---|---|---|---|---|---|---|---|---|---|
| Saint Catherine | 5.7 | 6.9 | 9.1 | 13.4 | 15.6 | 18.2 | 16.6 | 15.9 | 13.4 | 10.7 | 6.9 | 6.2 | 11.55 |
| El Tor | 7.2 | 8 | 9.5 | 11.1 | 12 | 12.5 | 12 | 11.9 | 11 | 8.2 | 7.5 | 7.3 | 9.85 |
| Sharm El Shiekh | 11.1 | 13.2 | 14.7 | 17.6 | 21 | 26.8 | 25 | 22.6 | 21.1 | 16.4 | 13 | 11.7 | 17.85 |

comparing the constructed hydrograph with the field-based hydrograph. Unfortunately, the WDB is lacking in-situ field data in order to achieve this verification step. To solve this dilemma, available field data was used from a nearby sub-basin, Wadi El-Sheikh is located in the neighbouring Wadi Feiran Basin to the west of the WDB. Wadi Dahab and Wadi El-Sheikh have similar topographical and geological characteristics (Omran 2013). The elevation of Wadi El-Sheikh ranges between 1207 and 2606 m above mean sea level. It received a low rainfall storm event (11 mm) in October 1993. This event was recorded at a local rainfall station in the catchment area of Wadi El-Sheikh with a duration of about 5 h (SSRDP 2006). The surface runoff was measured by a local runoff station at the outlet of Wadi El-Sheikh. Being similar to the WDB, the hydrological model was applied to Wadi El-Sheikh and the simulation results were compared against a field measured hydrograph.

The performance of the hydrological model (HEC-HMS) was evaluated against measured hydrograph data using two standard coefficient metrics, namely root mean square error (RMSE) and the correlation coefficient ($r$). The RMSE measures the global fitness of a predictive model by measuring the difference between the predicted and the observed values. Generally, a lower RMSE indicates a better fit between the predicted and the observed values. RMSE of a sample of ($n$) measurements is defined as follows:

$$\mathrm{RMSE} = \sqrt{\frac{\sum_{i=1}^{n} (XOi - XPi)^2}{n}}, \tag{4}$$

where $O$ is the observed value, and $P$ is the modelled value.

The correlation coefficient ($r$) is a measure of the linear correlation between two variables $X$ and $Y$. The value of ($r$) ranges between $-1$ and $+1$, where values of $+1$ and $-1$ indicate perfect increasing and decreasing linear relationships between variables, respectively. A value of 0 implies that there is no linear correlation between the variables. The value of ($r$) is obtained by dividing the covariance of the observed and modelled values by the product of their standard deviations according to the following formula:

$$r_{xy} = \frac{\sum \left(xi - \bar{x}\right)\left(yi - \bar{y}\right)}{\sqrt{\sum \left(xi - \bar{x}\right)^2 \sum \left(yi - \bar{y}\right)^2}}, \quad (5)$$

where ($x_i$ and $y_i$) and ($\bar{x}$ and $\bar{y}$) are the individual sample points indexed with ($i$) and the mean values, respectively.

After adjusting the input parameters, the calibrated model was applied once again using the maximum storm value of 72.6 mm/day over selected five sub-basins that were classified as high-risk basins in the WDB. All hydrographs of the major watersheds from the hydrological model were extracted and used as an input data for the hydraulic simulation in the HEC-River Analysis System (HEC-RAS) module. With this module, the hydraulics of water flow in the main channels were simulated. Several flow boundary condition points were generated to define the upstream and the downstream boundaries. Additional data using the HEC-GeoRAS module, which is the interface software for HEC-RAS and ArcGIS, were integrated into the HEC-RAS model to run a flood simulation resulting in a flood inundation map.

### Land-use mapping

Additionally, a land-use map was generated to understand the existing urbanization patterns of the WDB. Building footprints of Dahab urban areas were extracted from the Open Street Map (OSM) database. As depicted in the workflow, the OSM data were converted to KMZ files and overlaid in Google Earth to identify and digitize the missing built-up areas including their infrastructure like roads in the OSM data. The flood inundation and the updated land-use maps were used for the vulnerability assessment step.

## Results and discussions

First, the analysis of WDB was initiated based on manual evaluation and processing of topographic maps of scale 1: 50,000. The tracing technique and the numbering of streams were carried out using six sheets of topographic maps. Second, the stream counts for each stream order after being extracted from the SRTM-DEM were compared to those extracted from the topographic maps in which they showed and presented good agreement. Table 2 shows the higher order streams (i.e., from 5 to 8th) have a very strong correlation with a score of 100%; this correlation begins to decrease in the lower order streams (i.e., from 1st to 4th). Table 2 also shows the number of streams for the lower order streams (i.e., from 1st to 4th) previously extracted from SRTM-DEM is higher than the number of the similar stream orders that were extracted from the topographic maps. Such difference can be attributed to two reasons: (1) the effect of the threshold value being used for stream extraction and separation from the DEM file; and (2) elimination of the human errors that usually occur in analyzing hydrographic basins that were extracted from topographic maps. Notably, the high evaluation percentage reflects an optimum threshold value to define the channel network throughout the study area (Omran et al. 2016).

Approximately 173 basins and sub-basins were identified and delineated based on their nested hierarchy as the flow of streams drain from basin to basin until the main stream basin is formed representing the downstream part of the WDB. These basins resemble the shape of a funnel, where all waters are collected by the fine tributaries from the upstream area of WDB, then discharged through a single point at the downstream location of Dahab area. As mentioned before, the WDB can be divided into seven major

**Table 2** Validation of extracted drainage network from SRTM against network extracted from topographic maps of scale 1:50,000

| Stream order | Number of extracted streams from SRTM | Number of extracted streams from topographic maps | Evaluation (%) |
|---|---|---|---|
| 1st | 6250 | 6010 | 96.1 |
| 2nd | 1479 | 1440 | 97.4 |
| 3rd | 416 | 377 | 90.6 |
| 4th | 101 | 90 | 89.1 |
| 5th | 24 | 24 | 100 |
| 6th | 6 | 6 | 100 |
| 7th | 2 | 2 | 100 |
| 8th | 1 | 1 | 100 |

sub-basins. Similarly, all these seven sub-basins was divided into smaller "sub-sub-basins".

The extracted drainage network from the morphometric analysis has eight stream orders (Table 2). This hierarchical order gives an idea about the size and strength of the streams in the WDB. Normally, streams lower than fourth order (i.e., < 4th) represent a headwater feeding larger streams, while streams from fourth order to sixth order represent a medium-sized stream. Moreover, streams higher than sixth order (i.e., > 6th) are assumed to be wider wadis (Briney 2017). According to Strahler (1964), the total stream length of a particular order is inversely proportional to stream order. As such, the total stream length of WDB is 4972 km, but the stream length of the highest stream order (i.e., 8th) is 22 km. The calculated mean stream length ratio ranges from 0.29 to 51.02. The value of mean stream length is increasing with the increasing number in the stream order. Such link indicates the maturity stage of the geomorphic development of the study area (Parveen 2012).

From the assessment of the morphometric parameters in the WDB, it can be concluded that most of the sub-basins in the study area do not show high potential for flash flooding in terms of overland flow. They still have the characteristics to create a flash flood, however, especially during the extreme rainfall events. Therefore, results are divided into three main categories regarding hazard risk possibilities (low, medium, and high). These are based on applying equal intervals in ascending order. A flood hazard map was generated showing the flood potentiality for each sub-basin throughout the WDB (Fig. 5). According to the flood hazard map, 37% of the basin area of WDB can be identified as a most hazardous area with a high possibility to create a flash flood. Sub-basins in Wadi Rimthy, Wadi Genah, Wadi El-Ghaieb, and Wadi Nasab are also recognized as a high-risk zone prone to flash flooding. Also, around 52% of the sub-basins can be identified of moderate potentiality and only 11% of the sub-basins have a low risk of flood hazard. These low-risk areas are generally located in the upstream parts of the WDB.

The highest amount of rainfall in one day is considered to be one of the important pieces of data for studying the distribution of effective rainfall in arid zones. Gereish (1998) stated that runoff in southern Sinai, a region including W. Dahab basin, results from storms providing more than 10 mm of rainfall. Therefore, this storm record can be considered as a critical minimum storm value for the creation of the possible runoff in the study area. The recurrence time for maximum storm records is also estimated. The results show that the return period of maximum rainfall (72.6 mm/day) in the study area to be once in more than 95 years, while the

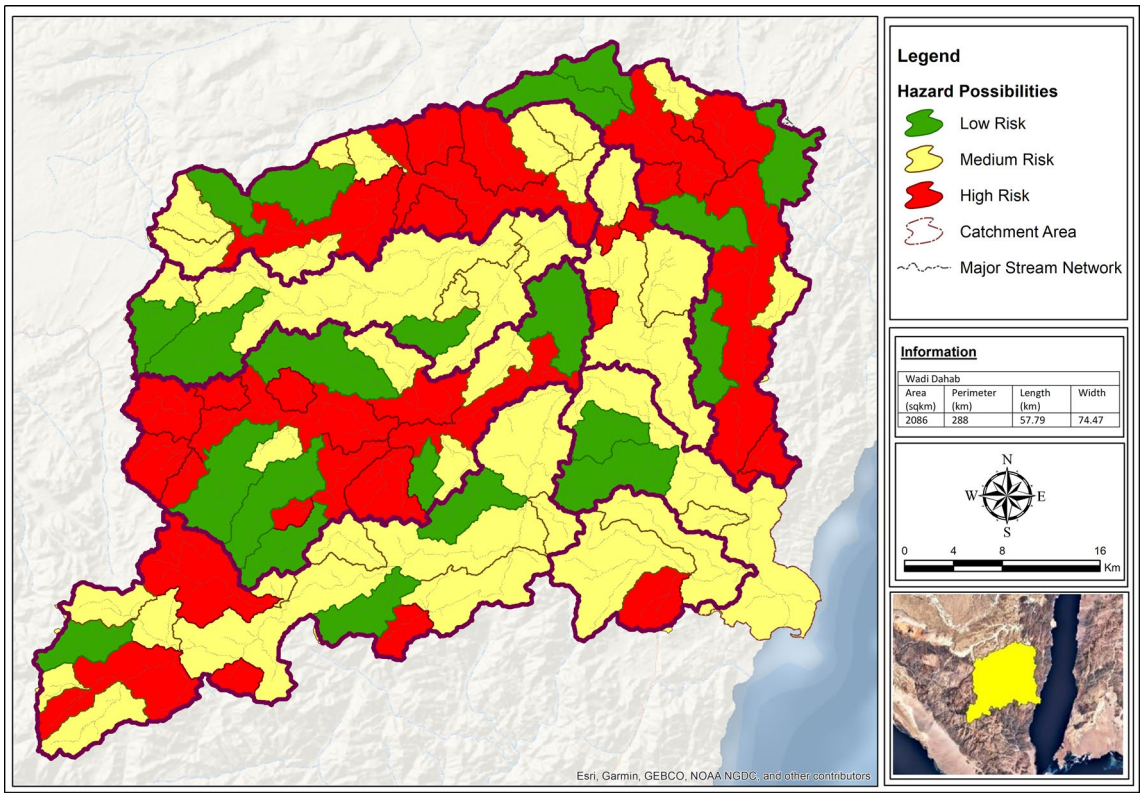


**Fig.5** Flood Hazard Map of the catchment area of WDB

minimum value recurrence for rainfall (10 mm/day) can be approximated to occur once every 3–4 years. This analysis illustrated that the maximum storm can be repeated with the next 20 years from now. These results have encouraged us to use this data in the runoff model combined with the availability of the measured hyetograph for corresponding maximum storm values.

Obviously, a runoff model converts the rainfall volume into surface runoff and then calculates the total possible discharge over a study area. Thus, the HEC-HMS is used in this regard to simulate the hydrologic processes of different watersheds using our extreme rainfall event (i.e., 72.6 mm/day). The model creates a hydrograph, which contains information about surface runoff for each sub-basin in the study area based on a specified simulation time interval. It also generates simulation data that include values of the area, peak discharge, and direct runoff volume. Results show that Wadi Zaghraa and Wadi El Ghaieb have the highest runoff volume among other Wadis with values equal to 37 and 17 million $m^3$, respectively. The values of peak discharge range from 126 to 709 $m^3/s$. Moreover, simulation results were calibrated and validated with measured field data by cross-checking to verify the accuracy of the model.

The model parameters were tested at the outlet of Wadi El-Sheikh with a low rainfall event of 11 mm/day. The peak discharge runoff measured at the outlet of Wadi El-Sheikh was 2.7 $m^3/s$ while the modeled discharge was 11.70 $m^3/s$. This indicates that the simulated hydrological model for Wadi El-Sheikh and consequently WDB requires significant adjustment. The curve number (CN) value was considered a critical parameter for the calibration correction. After running the simulation with different CN range values, the calibrated model of Wadi El-Sheikh matched with the field measured hydrograph with a CN value of 86 (Fig. 6a). After assigning the adjusted CN, the simulation results in (Table 3) showed that Wadi El-Sheikh yielded a peak discharge of 3.1 $m^3/s$ which produces a satisfactory approximate to the field measured hydrograph with a peak discharge of 2.7 $m^3/s$ showing that the time of peak is about 14.30 h. The modeled and measured hydrographs are highly correlated and characterized by a Pearson's correlation coefficient ($r$) of 0.86, and a root-mean-square error (RMSE) of 1.6 $m^3/sec$ (Fig. 6b).

The calibrated model was successfully applied to the WDB, particularly on the predefined risky sub-basins (i.e., high risk category). The model yielded different results compared to the non-calibrated model results (Table 4). Results show that Wadi Zaghraa is ranked first according to the peak discharge both before and after the calibration. Wadi Nasab and Wadi Rimthy have the potentiality to contribute more in flash flooding volume with a discharge rate ranging between 392 and 372 $m^3/s$, respectively. Also, Wadi El-Ghaieb and Wadi Abu Khashieb have lower discharge rates and less potentiality for flash flooding than the other major sub-basins. But Wadi Abu Khshieb is still considered

**Table 3** Simulation results of different parameter form the modelled and measured hydrograph at the outlet of Wadi El-Sheikh

| Precipitation data | Parameter | Modelled | Field measured |
|---|---|---|---|
| October 1993 | Peak flow ($m^3/s$) | 3.1 | 2.7 |
| | Time of peak flow (hr) | 14:20 | 14:30 |
| | Base time (hr) | 12:48–18:00 | 13:00–16:00 |
| | Volume ($m^3$) | 10,240 $m^3$ | 8960.4 $m^3$ |

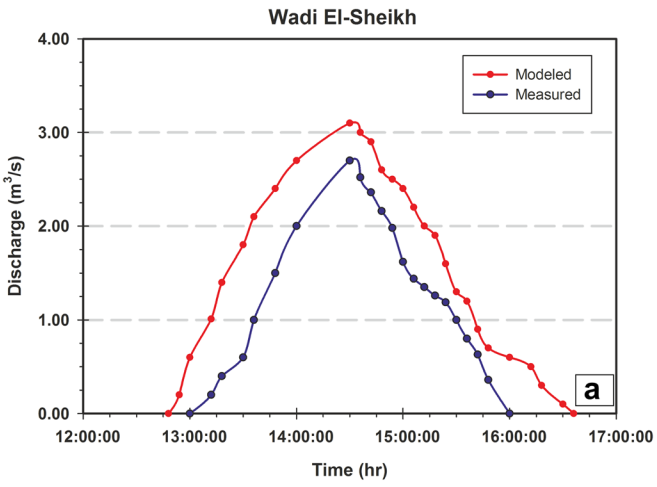


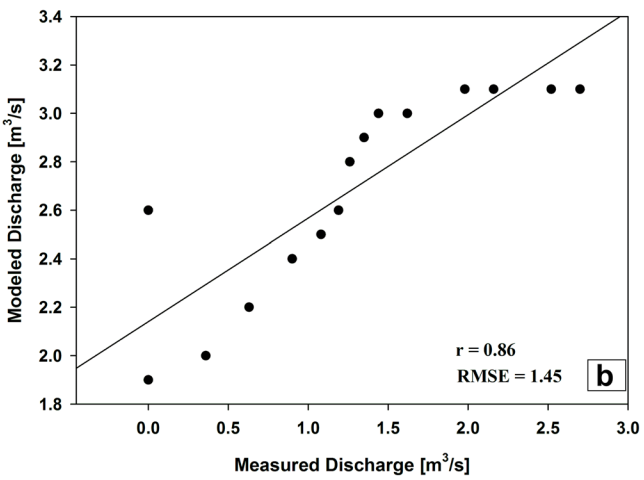


**Fig. 6** **a** Field measured hydrograph data compared to model simulation results over Wadi El Shiekh outlet in October 1993. Blue and red lines show the measured and modeled discharge in ($m^3/s$), respectively. **b** Validation of the model discharge output from the HEC-HMS against in-situ measured discharge data at Wadi El-Sheikh basin

**Table 4** Simulation result for major sub-basins in WDB before and after calibration

| Name | Hydrologic element | Drainage area ($km^2$) | Before model calibration | | After model calibration | | |
|---|---|---|---|---|---|---|---|
| | | | Peak discharge ($m^3/s$) | Volume (1000 $m^3$) | Peak Discharge ($m^3/s$) | Time to peak (h) | Volume (1000 $m^3$) |
| Wadi Zaghraa | Subbasin | 661.6 | 708.8 | 37,000.2 | 555.8 | 16:03 | 28,672.7 |
| Wadi Nasab | Subbasin | 444.22 | 503.4 | 24,910.4 | 391.6 | 13:54 | 19,311.4 |
| Wadi Rimthy | Subbasin | 413.39 | 413.4 | 23,184.7 | 371.9 | 13:18 | 17,973.9 |
| Wadi El Ghaieb | Subbasin | 297.2 | 333.9 | 16,663.9 | 259.7 | 14:18 | 12,918.2 |
| Wadi Abu Khashieb | Subbasin | 106.7 | 126.3 | 5984,4 | 100.9 | 12:18 | 4639.4 |

a potential source for flash flooding because of its proximity to the city of Dahab.

For conducting a vulnerability assessment study, the urbanization trend of the Dahab area was determined and analyzed using time-lapse imagery collected from Google Earth (Fig. 7). The Wadi channel divides the area of Dahab into the southern and northern parts. The latter is located in the old city with local Bedouin settlements, also known as the Bedouin Fishing Village. According to the image from 2004, the urban development in Dahab has mainly concentrated nearby to the Gulf of Aqaba and farther away from the main Wadi channel (Fig. 7). After 3 years (i.e., in 2007), there were significant changes in the northern urban area. The city experienced rapid urbanization within a short period of time. The rapid growth has resulted in a new settlement area (~4 $km^2$) where it has started expanding towards the central area of Dahab and it is located at the pathway of the main channel of WDB followed by the Gulf of Aqaba.

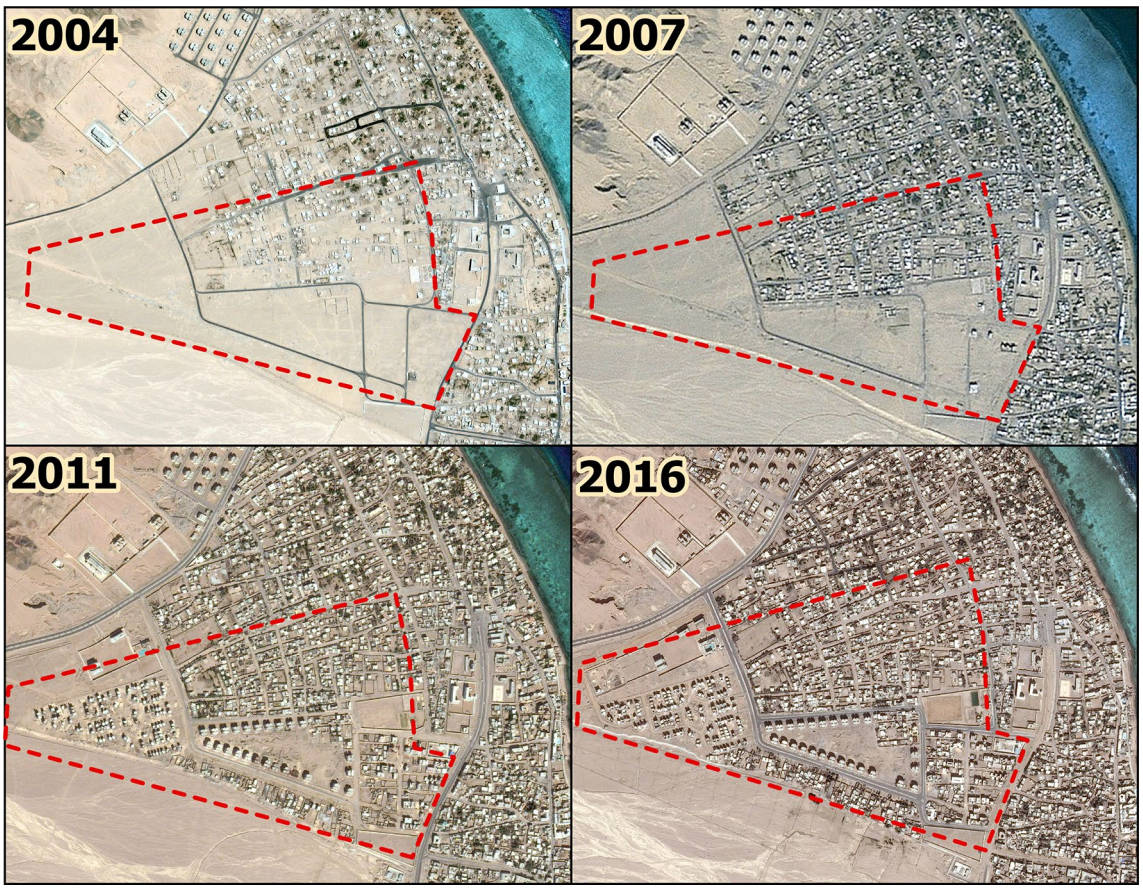


**Fig. 7** Trend of urbanization in the city of Dahab. Source: Time-lapse images from Google Earth (red rectangle outlines the urban settlements in the northern part of Dahab)

Until 2016, the Dahab city has grown in a manner where urban settlements expanded closer to the main outflow channel of the WDB.

The area outlined in red, Fig. 7 shows the newly constructed urban settlement area in Dahab from 2004 to 2016. It is clearly visible that the newly urbanized area is very close to the main channel of WDB allowing it to be directly exposed and threaten by the flash flooding waters. Normally, urbanization comes with good economic prospects, in addition to cultural and social development. However, having a closer look at the urban development in Dahab shows a threat to human life. This assumption is evidenced after overlaying the inundation map on top of the land-use map (Fig. 8). Here, the inundation map was successfully created in the HEC-RAS using the hydraulic information such as the water depth and velocity originating from a specific flood event. The hydraulic modeling in the HEC-RAS can simulate these parameters for a flood event.

The flood simulation in HEC-RAS demonstrates that the central part of the city of Dahab is highly vulnerable to flash flooding. It has already been mentioned that the central area of Wadi Dahab carries all of the accumulated flood water collected into the main course of the Wadi and discharges it into the Gulf of Aqaba (SSRDP 2006). After the fusion of the land-use data with the inundation map, the 0.26 $km^2$ of the newly urbanized area within Dahab is obviously highly vulnerable to flash flooding (Fig. 9). As determined by the flood simulation, the maximum flood depth is about 4.5 m. This maximum impacts various points along the main channel especially along the central city portion of Dahab and indicates that the central part of Dahab is highly vulnerable to flash flooding when there is a relatively high volume of surface runoff.

The inundation map represents the area of most probable inundation from a specific flood event. After overlaying the land-use map with the inundation map, infrastructures can be identified as the most prone areas that can be impacted by direct surface runoff and flash flooding (see Fig. 7, marked in red). In the northern and southern parts of the city, average water depth is between 0 to 1 m. It can be concluded that the northern part of the city is more vulnerable because of its dense urbanization. The dense urbanization decreases the infiltration rates as it consists of a built-up impervious surface. As such, the impervious surface increases the overland flow velocity subsequently increasing the flow rate (Zhang et al. 2008). Additionally, the northern part of Dahab represents the old area of the city where the old residential buildings are usually constructed without adequate foundation (SSDP 2006). This indicates that a few hours of flash flooding with high

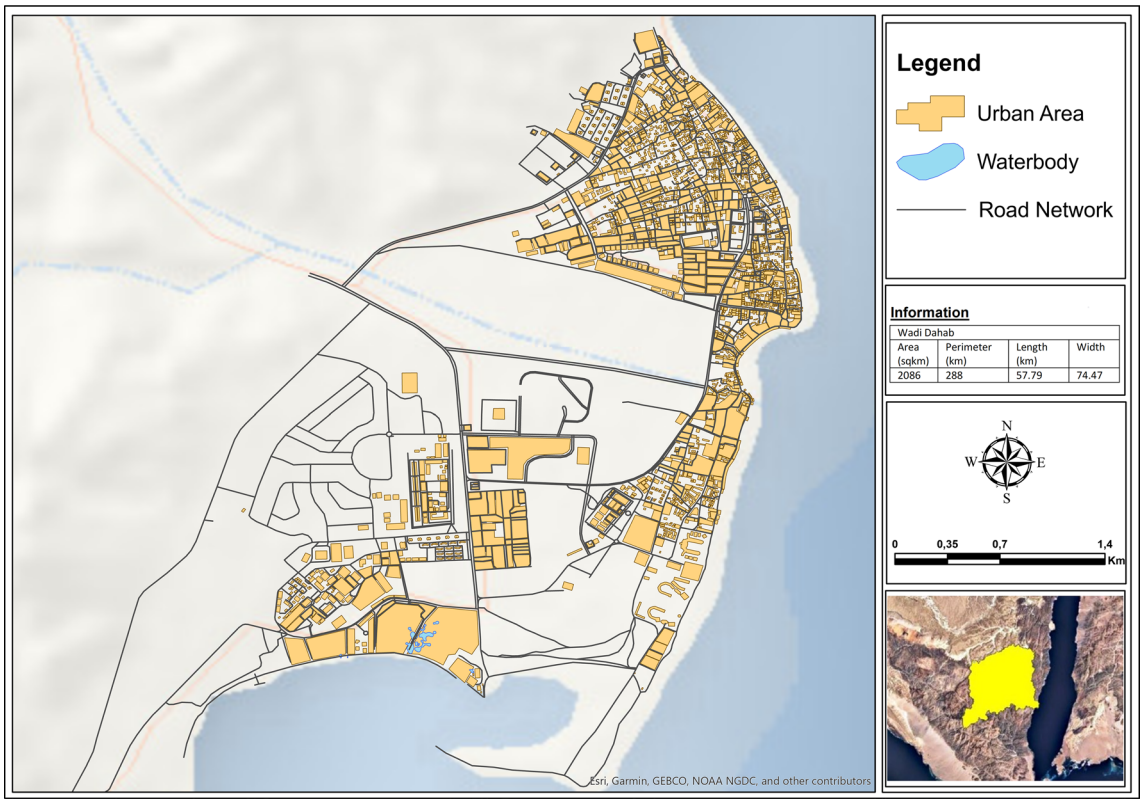


**Fig. 8** Land-use map of the city of Dahab

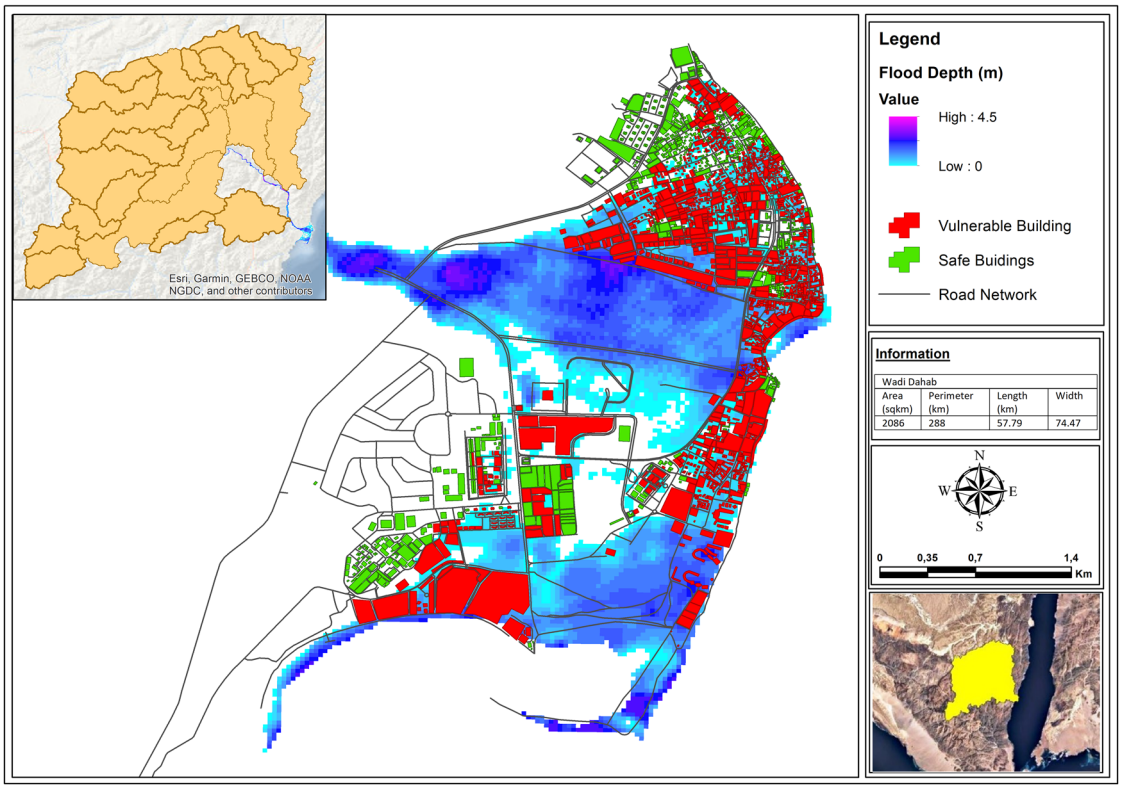


**Fig. 9** Physical vulnerability relevant to flash flood in the city of Dahab

volume and relatively high velocity may cause severe consequences such as the collapse of buildings, destruction of infrastructures, and threatening human lives.

The southern part of Dahab is the newly developed area. According to the flood vulnerability map (Fig. 9), this part of the city is less prone to flash flooding compared to the northern part. However, the width of the outlet points of the Wadi's main channel towards the Gulf of Aqaba has been reduced from 500 to 30 m by the expansion of the buildings causing considerable restrictions to the natural water flow. Thus, the depth of the water rises in this area simultaneously increasing the possible damage to the urban infrastructure and road networks. Ironically, the main road of the city of Dahab follows the course of the Wadi Dahab's main channel making it highly vulnerable to flash flooding. The damage to the main road would hinder the regular communication capacity as well as the traffic and tourism activities. Actually, the entire tourism industry of Dahab area is vulnerable to the impact of flash flooding because the flooded water would severely affect hotels and other business activities comprising the main economic resources of the city. Therefore, the flooding is a threat not only to the physical features of the city but also to the entire economy of the city.

## Conclusions and summary

The city of Dahab is vulnerable to flash flooding based on our findings produced through the adopted approach utilizing the use of (1) the morphometric analysis; (2) the digital data sets acquired from satellite-based remote sensing; (3) the flood hazard map, and (4) the hydrological simulation using the runoff model HEC-HMS. The results of the morphometric analysis indicate that most of the sub-basins in the WDB have a high potentiality to contribute to the risk of flash flooding, especially to the urbanized areas of Dahab. The hydrological simulation is strongly matched with the results from the flood hazard map demonstrating that the main sub-basins of Wadi Zaghraa, Wadi El-Ghaieb, and Wadi Abu Khashieb can be considered the riskiest sub-basins in the WDB in that they could directly impact the Dahab area. Also, the combined overlay of the inundation map from the HEC-RAS and the land-use map

shows that the major part of the current urban development area is directly affected by flash flooding.

The land-use map shows that around 72% of the total infrastructure in the city of Dahab is vulnerable to flash floods that were generated from the highest precipitation value of 72.6 mm/day. The inundation map has confirmed that the major part of the city would be inundated with mean depths ranging from 1.0 to 1.5 m. The construction cost in the city of Dahab has been estimated to be around 300 Euro/$m^2$ (SSRDP 2006). Therefore, the expected economic damage to the city would cost around 41 million Euros if the city were to be impacted by a severe flash flood. Additionally, the overall economy will be influenced on a large scale—about 62% of the total economy of Dahab—as it depends primarily on the tourism sector, which would be severely affected by such a flood (SSRDP 2006). Afterward, the flood event also pulls downwards the production efficiency until normalization of the situation is accomplished. This may have an even greater impact on the annual economic totals.

As an outcome of the data limitation for this study, we could not determine the quantitative physical vulnerability in detail. However, we were able to apply vulnerability assessment in the research, identify the hazard impact on Dahab, and recognize the mitigation measurement demand for sustainable development. A probable measurement would be to consider those issues in urban planning and applying some rules for safe urban development. The result of this study can be useful as a foundational database and guideline for the detailed assessment of risk components.

Relevant to this study, the vulnerability results lead to some recommendations for further urban development in Dahab. First, urban development in the central part of Dahab should be restricted. Second, the southern part of the city looks comparatively safer than the northern part of the city. Therefore, we recommend that future urbanization should be focused on the southern part of the city for safer urban development. Additionally, further development in the surrounding area of the flood outlet point should be restricted. This may be helpful to allow the flash flood water to flow without interruption and reduce the vulnerability of coastal development. The existing dams in the study area were investigated to test their efficiencies using GIS tools and field checking (Omran 2013). These dams were constructed by Water Resources Research Institute (WRRI) in Wadi El-Ghaieb and Wadi El-Genah in 2006 to protect the main road between Dahab and Nuweiba. A new protection system has been proposed by (Omran 2013) to upgrade the current protection level and increase its storage efficiency in order to protect the local inhabitants (Bedouins) and main infrastructures in Dahab basin against floods. To protect the area of the WDB from flash floods, the following should be taken into consideration: (1) protection tools such as retention dams for the Delta of the WDB should be applied at the headwater area of the basin; (2) implementing commonly used structures such as detention dams, cisterns, mitigation canals are highly recommended in order to mitigate the effects of flash floods, store water behind these dams, and augment the existing groundwater aquifers. The use of these structures is of prime importance in the sustainable development strategy for the city of Dahab on a local scale and for other comparable cities in the Sinai Peninsula and elsewhere.

We believe that our approach is robust and advantageous for the following reasons: (1) it was successfully tested over Wadi Dahab Basin and it could potentially be applied to similar basins in the Sinai Peninsula and other comparable basins having similar geological and climatic conditions, (2) it could be applied to relatively large hydrographic basins in the basement terrain environments, and (3) it provides unprecedented results in remote locations that are lacking an adequate density of monitoring systems.

**Acknowledgements** Open Access funding provided by Projekt DEAL. The authors would like to thank the Department of Photogrammetry and Geoinformatics in Hochschule für Technik Stuttgart, the Heidelberger Akademie für Wissenschaften, the Water Resources Research Institute (WRRI) in Egypt and the Geographische Institute at Universität Tübingen for providing relevant data and support to complete this study.



## References

Abdel-Fattah M, Saber M, Kantoush S, Khalil F, SumiT SA (2017) A hydrological and geomorphometric approach to understanding the generation of wadi flash floods. Water 9:553. https://doi.org/10.3390/w9070553

Abdalla F, El-Shamy I, Bamousa A, Mansour A, Mohamed A, Tahoon M (2014) Flash floods and groundwater recharge potentials in arid land alluvial basins, southern red sea coast, Egypt. Int J Geosci 5:971–982. https://www.scirp.org/journal/ijg **(10.4236/ijg.2014.59083)**

Abuzied S, Yuan M, Ibrahum S, Kaiser M, Saleem T (2016) Geospatial risk assessment of flash floods in Nuweiba area. Egypt JArid Environ 133:54–72

Abdel-Fattah M, Kantoush S, Sumi T (2015) Integrated management of flash flood in wadi system of Egypt: disaster prevention and

water harvesting. First international symposium on flash floods in wadi System—disaster risk reduction and water harvesting of flash floods in the Arab Regions 14–15 October. https://www.dpri.kyoto-u.ac.jp/nenpo/no58/ronbunB/a58b0p54.pdf. Accessed 10 Jan 2017

Adham M, Shirazi S, Othman F, Rahman S, Yusop Z, Ismail Z (2014) Runoff potentiality of a watershed through SCS and functional data analysis technique. Sci World J. https://doi.org/10.1155/2014/379763

Adib A, Salarijazi M, Najafpour K (2010) Evaluation of synthetic outlet runoff assessment models. J Appl Sci Environ Manag 14.

Altaf F, Meraj G, Romshoo SA (2013) Morphometric analysis to infer hydrological behaviour of Lidder Watershed, Western Himalaya India. Geogr J 2013:14

Al-Qudah KA (2011) Floods as water resource and as a hazard in arid regions: a case study in southern Jordan. Jordan J Civil Eng 5(1):148–161

Antwi EK, Danquah JB, Owusu AB, Loh SK, Mensah R, Boafo YA et al (2015) Community vulnerability assessment index for flood prone savannah agro-ecological zone: a case study of Wa West District, Ghana. Water Clim Extrem 10:56–69

Bhatt S, Ahmed SA (2014) Morphometric analysis to determine floods in the Upper Krishna Basin using Cartosat DEM. J Geocarto Int 29(8):878–894. https://doi.org/10.1080/10106049.2013.868042

Briney A (2017) Stream order—a classification of the rank of stream and rivers. https://www.thoughtco.com/what-is-stream-order-1435354. Accessed 16 Jan 2017

Chorley RJ, Schumm SA, Sugden DE (1984) Geomorphology. Methuen, London, p 605

Choudhari K, Panigrahi B, Paul JC (2014) Simulation of rainfall-runoff process using HEC-HMS model for Balijore Nala watershed, Odisha India. Int J Geomat Geosci 5(2):253–265

Cools J, Vanderkimpen P, Afandi GE, Abdelkhalek A, Fockedey S, Sammany ME et al (2012) An early warning system for flash floods in hyper-arid Egypt. Nat Hazards Earth Syst Sci 12:443–457. https://doi.org/10.5194/nhess-12-443-2012

Crane E (2015) The rising danger of flooding in Egypt. https://climate.earthjournalism.net/2015/12/07/extreme-rainstorms-sweep-through-egypt/. Accessed 10 Jan 2017

Davies R (2014) World disaster report—most deaths caused by flood. https://floodlist.com/dealing-with-floods/world-disasters-report-100-million-affected-2013. Accessed 6 Oct 2016

El-Magd IA, Hermas E, Bestawesy M (2010) GIS-modeling of the spatial variability of flash flood hazard in Abu Dabbab catchment, Red Sea Region Egypt. Egypt J Remote Sens Space Sci 13(1):81–88. https://doi.org/10.1016/j.ejrs.2010.07.010

Farhan Y, Anaba O, Salim A (2016) Morphometric Analysis and flash floods assessment for drainage basins of the Ras En Naqb Area South Jordan Using GIS. J Geosci Environ Protect. https://doi.org/10.4236/gep.2016.46002

Fuchs S (2009) Susceptibility versus resilience to mountain hazards in Austria—paradigms of vulnerability revisited. Nat Hazards Earth Syst Sci 9(2):337–352

Geriesh H (1998) Artificial recharge as an effective tool for augmenting the natural groundwater resources in Saint Katherine area, South Sinai, Egypt. In: Proceedings of the 5th conference Geol. Sinai development, Suez Canal University, Ismailia, p. 47–64.

Google Maps (2017) Google Maps. [online] Available at: https://www.google.com.au/maps/@-23.3394728,150.5201386,12z?hl=en.

Gumindoga W, Rwasoka D, Nhapi I, Dube T (2016) Ungauged runoff simulation in Upper Manyame Catchment, Zimbabwe: application of the HEC-HMS model. Phys Chem Earth Parts A/B/C. https://doi.org/10.1016/j.pce.2016.05.002

Guisti E, Schneider W (1965) The distribution of branches in river network. Geological Survey Professional Paper 422-G, United Sates Department of The Interior. https://pubs.usgs.gov/pp/0422g/report.pdf. Accessed 20 Oct 2016

Hagras MA, Elmoustafa AM, Kotb A (2013) Flood plain mitigation in arid regions case study: south of Al. Kharj City, Saudi Arabia. Int J Res Rev Appl Sci 16(1), 147–156.

Hajam RA, Hamid A, Bhat S (2013) Application of morphometric analysis for geo-hydrological studies using geo-spatial technology—a case study of Vishav Drainage Basin. Hydrol Curr Res 4(3):1–12. https://doi.org/10.4172/2157-7587.100015

Hong WS, Tao P, Feng HS (2012) Climate change risk research: a case study on flood disaster risk in China. Adv Clim Change Res 3(2):92–98

Horton R (1945) Erosional development of streams and their drainage basins: hydrophysical approach to quantitative morphology. Geol Soc Am Bull 56:275–370. https://doi.org/10.1130/0016-7606(1945)56[275:EDOSAT]2.0.CO;2

Jadhav I, Babar MD (2014) Linear and aerial aspect of basin morphometry of kundka sub-basin of Sindphana Basin (Beed), Maharashtra, India. Int J Geol Agric Environ Sci 2(3):16–20

Jenson SK, Domingue JO (1988) Extracting Topographic Structure from digital elevation data for geographic information system analysis. Photogramm Eng Remote Sens 54(11):1593–1600

Jhariya G, Ramjan R, Jaiswal RK (2014) Morphological analysis of bina river basin using GIS and remote sensing. In: 4th international conference on hydrology and watershed management: ecosystem resilience-rural and urban water requirements, India. pp 206–214

Jin H, Liang R, Wang Y, Tumula P (2015) Flood—runoff in semi-arid and sub-humid regions, a case study: a simulation of Jianghe Watershed in Northern China. Water 7:5155–5172. https://doi.org/10.3390/w7095155 **(Accessed 10 January 2017)**

Karagiorgos K, Thaler T, Heiser M, Hübl J, Fuchs S (2016) Integrated flash flood vulnerability assessment: insights from East Attica, Greece. J Hydrol 541(A): 553–562. doi: 10.1016/j.jhydrol.2016.02.052.

Kim ES, Choi H (2011) Assessment of vulnerability to extreme flash floods in design storms. Int J Environ Res Public Health 8(7):2907–2922

Koneti S, Sunkara S, Roy P (2018) Hydrological modeling with respect to impact of land-use and land-cover change on the runoff dynamics in Godavari River Basin using the HEC-HMS Model. ISPRS Int J Geo Inf 7(6):206. https://doi.org/10.3390/ijgi7060206

Kundzewicz ZW, Kaczmarek Z (2000) Coping with hydrological extremes. J Water Int 25(1):66–75. https://doi.org/10.1080/02508060008686798

Lin X (1999) Flash floods in arid and semi-arid zones. UNESCO, Paris, p 65

Ludwig R, Schneider P (2006) Validation of digital elevation models from SRTM X-SAR for applications in hydrologic modelling. ISPRS J Photogramm Remote Sens. https://doi.org/10.1016/j.isprsjprs.2006.05.003

Mazzorana B, Simoni S, Scherer C, Gems B, Fuchs S, Keiler M (2014) A Physical approach on flood risk vulnerability of buildings. Hydrol Earth Syst Sci 18:3817–3836. https://doi.org/10.5194/hess-18-3817-2014 **(Accessed 15 Jan 2017)**

Mockus V (1972) National engineering handbook, section 4, chapter 7: hydrologic soil groups. US Department of Agriculture, Washington

Nandalal H, Ratnayake R (2010) Event based modeling of a watershed using HEC-HMS. Engineer XXXXIII(02):28–37

Nasiri H, Yusof MJM, Ali TAM (2016) An Overview to flood vulnerability assessment methods. Sustain Water Resour Manag 2(3):331–336. https://doi.org/10.1007/s40899-016-0051-x **(Accessed 20 Dec)**

National Flood Programs and Policies Review (2007) Arid regions hazards, resources and issues. National flood programs and policies in

review, pp 62–63. https://www.floods.org/PDF/ASFPM_NFPPR_2007.pdf. Accessed 28 Dec 2016
Neto AR, Scott AA, Lima EA, Montenegro SMGL, Cirilo JA (2014) Infrastructure sufficiency in meeting water demand under climate-induced socio-hydrological transition in the urbanizing capibaribe River Basin—Brazil. Hydrol Earth Syst Sci 18(9):3449–3459. https://doi.org/10.5194/hess-18-3449-2014
Noori N, Kalin L, Srivastava P, Lebleu C (2011) Effects of initial abstraction ratio in SCS-CN method on modeling the impacts of urbanization on peak flows. In: World environmental and water resources congress 2012: cross boundaries, Albuquerque, New Mexico, United States, pp: 1–12. https://doi.org/10.1061/9780784412312
OCHA (2016) Egypt: floods – Oct 2016. Relief Web. https://reliefweb.int/disaster/fl-2016-000114-egy/thumb#content_top. Accessed 22 Dec 2016
Omran A (2013) Application for GIS and Remote sensing for water resource management in Arid Area-Wadi Dahab Basin-South Eastern Sinai-Egypt (Case Study). Dissertation, University of Tübingen, Germany.
Omran A, Schröder D, El Rayes A, Geriesh M (2011) Flood hazard assessment in Wadi Dahab Based on Basin Morphometry using GIS Techniques. GI_Forum Symposium and Exhibit applied Geoinformatics, Salzburg, Austria, Wichman, pp 1–11
Omran A, Schröder D, Abouelmagd A, Märker M (2016) New ArcGIS tools developed for stream network extraction and basin delineations using Python and Java Script. Computer & Geoscience, Elsevier 94, p. 140–149. https://www.deepdyve.com/lp/elsevier/new-arcgis-tools-developed-for-stream-network-extraction-and-basin-dIC9VmzVoz
Pierson SM, Rosenbaum BJ, Mckay LD, Dewald TG (2008) Strahler Stream Order and Strahler Calculation Values in NHD Plus. United States Geological Survey. ftp://ftp.horizon-systems.com/NHDPlus/NHDPlusV1/NHDPlusExtensions/SOSC/SOSC_technical_paper.pdf Accessed 20 Dec 2016.
Pal B, Samanta S, Pal DK (2012) Morphometric and hydrological analysis and mapping for watut watershed using remote sensing and GIS techniques. Int J Adv Eng Technol 1(6):357–368
Palaka R, Sankar GJ (2014) Study of watershed characteristics using Google Elevation Service Geospatial Forum Hyderabad. https://www.researchgate.net/publication/260595644_Study_of_Watershed_Characteristics_using_Google_Elevation_Service. Accessed 20 Jan 2017
Parveen R, Kumar U, Singh VK (2012) Geomorphometric characterization of upper south koel basin, Jharkhand: a remote sensing and GIS approach. J Water Resour Protect 4(12):1042–1050. https://doi.org/10.4236/jwarp.2012.412120
Patel (2016) SCS Runoff Curve Number Method. https://www.professorpatel.com/curve-number-introduction.html. Accessed 12 Nov
Ponce VM, Magallon L (2015) Initial abstraction revisited. https://ponce.sdsu.edu/initial_abstraction_revisited.html Accessed 2 Oct 2016
Pradhan B (2010) Flood susceptible mapping and risk area delineation using logistic regression, GIS and remote sensing. J Spatial Hydrol 9(2):1–18
Rahman SA, Ajeez SA, Aruchamy S, Jegankumar R (2015) Prioritization of sub-watershed based on morphometric characteristics using fuzzy analytical hierarchy process and geographical information system—a study of kallar watershed Tamil Nadu. Int Conf Water Resour Coast Ocean Eng 4:1322–1330. https://doi.org/10.1016/j.aqpro.2015.02.172
Scharffenberg B (2004) Official HEC-HMS introduction. US Army Corps of Engineers Hydrologic Engineering Center
Sharma A, Tiwari KN (2014) A comparative appraisal of hydrological behavior of SRTM DEM at catchment level. J Hydrol. https://doi.org/10.1016/j.jhydrol.2014.08.062
Sidral A, Zende A (2016) Quantitative Evaluation of Morphometric Parameters of Sakli River Using Geospatial Techniques. In: National Conference on water resource and flood management with special reference of flood modeling, 14–15 October
Sing P, Gupta A, Singh M (2014) Hydrological inferences from watershed analysis for water resource management using remote sensing and GIS techniques. Egypt J Remote Sens Space Sci 17(2):111–121. https://doi.org/10.1016/j.ejrs.2014.09.003
SSRDP-South Sinai Regional Development Programme (2006) Architectural and engineering services for the flood protection of the City of Dahab in South Sinai. The Arab Republic of Egypt
Strahler AN (1957) Quantitative analysis of watershed geomorphology. Trans Am Geophys Union 38:913–920
Strahler AN (1964) Quantitative geomorphology of drainage basins and channel networks. In: Chow VT (ed) Handbook of applied hydrology. McGrawHill, Newyork, p 411
Sujatha ER, Selvakumar R, Rajasimman UAB, Victor RG (2013) Morphometric analysis of sub-watershed in parts of Western Ghats, South India using ASTER DEM. Geomat Nat Hazard Risk 6(4):326–341. https://doi.org/10.1080/19475705.2013.845114
Talukdar R (2011) Geomorphological study of the JiaBharali River catchment N E India. Dissertation, Gauhati University, Guwahati.
UNISDR (2009) Terminologies on disaster risk reduction United Nations International Strategy for Disaster Reduction Geneva, Switzerland
USDA-United States Department of Agriculture (1993) National Engineering Handbook. Section 4: Part 630, Hydrologic Engineering. Soil Conservation Services, United States government
USDA-United States Department of Agriculture (1986) Urban Hydrology for Small Watersheds. United States, Technical Release 55, Conservation Engineering Division. https://www.nrcs.usda.gov/Internet/FSE_DOCUMENTS/stelprdb1044171.pdf. Accessed 10 Feb
Vanderkimpen P, Rocabado I, Cools J, El-Sammany M, Abdelkhalek A (2010) FlaFloM – an early warning system for flash floods in Egypt. WIT Trans Ecol Environ 133:193–202
Wagener T, Gupta H, Yatheendradas S, Goodrich D, Unkrich C, Schaffner M (2007) Understanding sources of uncertainty in flash-flood forecasting for semi-arid region. Quantification and Reduction of predictive uncertainty for sustainable resources management-24th General Assembly of the International Union of Geodesy and Geophysics (IUGG), Italy, pp 204–212. https://citeseerx.ist.psu.edu/viewdoc/download?doi=10.1.1.504.3644&rep=rep1&type=pdf Accessed 2 Jan 2017
Waikar ML, Nilawar AP (2014) Morphometric analysis of a drainage basin using geographical information system: a case study. Int J Multidiscip Curr Res 2:179–184
Wicht M, Skotak KO (2016) Identifying urban areas prone to flash flood using GIS-preliminary results. Hydrol Earth Syst Sci. https://doi.org/10.5194/hess-2016-518 **(Accessed 10 Jan 2017)**
Windarto J (2010) Flood early warning system develop at garang river semarang using information technology base on SMS and web. Int J Geomat Geosci 1(1):14–28
Youssef AM, Sefry SA, Pradhan B, Alfadail EA (2016) Analysis on causes of flash flood in Jeddah city (Kingdom of Saudi Arabia) of 2009 and 2011 using multi-sensor remote sensing data and GIS. Geomat Nat Hazards Risk 7(3):1018–1042. https://doi.org/10.1080/19475705.2015.1012750
Zhang H, Ma W, Wang XR (2008) Rapid urbanization and implementations for flood risk management in hinterland of the Pearl River Delta, China: the Foshan Study. Sensors 8(4): 2223–2239. https://www.mdpi.com/1424-8220/8/4/2223. **(Accessed 10 Dec 2016)**